Progress In Electromagnetics Research, PIER 28, 253–273, 2000

NONUNIFORM FAST COSINE TRANSFORM AND CHEBYSHEV PSTD ALGORITHMS

B. Tian and Q. H. Liu

Department of Electrical and Computer Engineering
Duke University
Durham, NC 27708, USA

1. INTRODUCTION

In this work our main interests are to develop fast cosine transform algorithms that are applicable to nonuniformly spaced data, and to use these algorithm to improve the numerical solution of time-domain Maxwell's equations.

Fast cosine transform (FCT) has many applications in signal processing and computational electromagnetics. There are several well-developed efficient FCT algorithms [1–3]. The basic assumption of the regular FCT algorithms is that the input data has to distribute uniformly. In reality, however, the nonuniform data is common in many applications. The nonuniformity may be a result of sampling error, of

convenience, or by intention. For example, to solve a wave propagation problem in a medium with both electrically large and small regions, it is more efficient to sample nonuniformly. Under these circumstances, regular FFT or FCT algorithms do not apply. Unfortunately, the direct summation of the nonuniform discrete cosine transform (NUDCT) costs $O(N^2)$ arithmetic operations, where N is the number of sample points.

Following the idea of fast interpolation for the nonuniform fast Fourier transform (NUFFT) algorithms [4–8], in this work we develop nonuniform fast cosine transform algorithms. In particular, we use the idea of least-squares interpolation of an exponential function on a nonuniform grid by some oversampled uniform points. During this interpolation, the regular Fourier matrices are derived [6, 8] which are independent of the nonuniform points. As a result, the interpolation can be performed efficiently. These algorithms have the complexity of $O(N \log_2 N)$.

For the nonuniform inverse cosine transforms, we find that the solution can be obtained by the iterative conjugate-gradient FFT method. That is, the matrix equation is solved iteratively by the CG method; while in each CG iteration the matrix vector multiply is achieved efficiently by the FFT algorithm for the convolution and correlation. The resulting inverse algorithm has a computational complexity of $O(KN \log_2 N)$ where K is the number of CG iterations.

The major application of the NUFCT algorithms is the numerical solution of time-dependent Maxwell's equations. Conventionally, the finite-difference time-domain method [9–11] is used to solve these partial differential equations with a second-order accuracy. Higher order finite-difference methods have also been used [12–15]. The Fourier and Chebyshev pseudospectral methods originally proposed by Kreiss and Oliger [16] and by Orszag [17] have been widely used [18]. Because of the implicit periodicity in the FFT, the Fourier pseudospectral method was used for periodic problem. The Chebyshev pseudospectral method is more widely used since it does not have such a limitation. For a medium with several regions, traditionally a multiregion approach is used so that each region is solved separated and boundary conditions are used across adjacent regions.

Recently the perfectly matched layer (PML) [19] has been used for both Fourier and Chebyshev pseudospectral methods [20–27]. It completely removes the limitation of the wraparound effect associated with

the Fourier pseudospectral method, and allows an effective modeling of an unbounded medium in the Chebyshev pseudospectral method. Following the convention of the FDTD method, we call these the Fourier and Chebyshev PSTD methods. For smooth fields, these methods require only two points and π points per wavelength, respectively, rather than 10–20 points per wavelength in the FDTD method even for a moderate-size problem. The advantage of the Chebyshev PSTD method over the Fourier PSTD method is that it can be used to model bounded media.

In this work, we proposed the application of our NUFCT algorithms in the Chebyshev pseudospectral time domain (PSTD) method for the solution of Maxwell's equations. Instead of treating multiple regions separately, this method allows the complete treatment of multiple regions simultaneously. This advantage becomes particularly attractive when there are many regions with significant different scales. Furthermore, for regions with different dielectric constants, this method allows us to sample differently from region to region so that the memory requirement is efficient.

This paper is organized as follows. We first present the forward and inverse fast cosine transform algorithms for nonuniformly sample data. Then as an application, we apply these algorithms to represent electromagnetic fields and their derivatives in order to solve the one-dimensional Maxwell's equations. Finally we present the numerical results for the NUFCT algorithms and the nonuniform Chebyshev PSTD method.

2. FORMULATION

2.1 Forward NUFCT Algorithm

For nonuniform points $c_k \in [0, N]$, two different discrete cosine transforms (DCT's) of real data α_k can be defined as:

$$\begin{aligned} f_j =& \sum_{k=0}^{N} \alpha_k \cos(k\pi c_j/N) \\ =& \Re e \left(\sum_{k=0}^{N} \alpha_k e^{i2\pi k c'_j/N} \right) = \Re e(\tilde{f}_j), \qquad j = 0, 1, 2, \ldots, N \end{aligned} \tag{1}$$

$$g_j = \sum_{k=0}^{N} \alpha_k \cos(j\pi c_k/N)$$
$$= \Re e\left(\sum_{k=0}^{N} \alpha_k e^{i2\pi j c'_k/N}\right) = \Re e(\tilde{g}_j), \qquad j = 0, 1, 2, \ldots, N \quad (2)$$

where $c_j = 2c'_j$. Here we refer to the fast algorithm for (1), which has nonuniform frequency points c_j, as NUFCT-1. Similarly, NUFCT-2 refers to the algorithm for (2), which has nonuniform time sample points c_k. Note that in order to use the regular Fourier matrices in [6], we have rewritten the cosine transforms as the real part of weighted summation of exponential functions. In general, the regular fast cosine transform algorithms do not apply. The direct summation of (1) and (2), unfortunately, costs $O(N^2)$ arithmetic operations.

Following the idea for the nonuniform fast Fourier transform (NUFFT) in [6], we interpolate an exponential function at nonuniform points with some oversampled uniform points. Introducing accuracy factor $s_k = \cos(k\pi/mN - \pi/2m)$ and interpolating each value of $s_k e^{i2\pi k m c'_j/mN}$ in terms of $(q+1)$ uniform points, we obtain

$$\tilde{f}_j \simeq \sum_{k=0}^{N} \beta_k \sum_{\ell=-q/2}^{q/2} x_\ell(c'_j) e^{i2k\pi([mc'_j]+\ell)/mN}, \quad (3)$$

$$\tilde{g}_j s_j \simeq \sum_{k=0}^{N} \alpha_k \sum_{\ell=-q/2}^{q/2} x_\ell(c'_k) e^{i2\pi j([mc'_k]+\ell)/mN}, \quad (4)$$

where $\beta_k = s_k^{-1}\alpha_k$, x_ℓ are interpolation coefficients, m is the oversampling rate, and $[mc'_j]$ denotes the integer nearest to mc'_j.

We first formulate the NUFCT-1 algorithm. We rearrange (3) as

$$\tilde{f}_j = \sum_{\ell=-q/2}^{q/2} x_\ell(c'_j) \sum_{k=0}^{N} \beta_k e^{ik\pi([mc'_j]+\ell)/mN} = \sum_{\ell=-q/2}^{q/2} x_\ell(c'_j)\mu\left([mc'_j]+\ell\right) \quad (5)$$

where

$$\mu\left([mc'_j]+\ell\right) = \sum_{k=0}^{N} \beta_k e^{i2k\pi([mc'_j]+\ell)/mN} \quad (6)$$

is the regular FFT of array β_k of length mN with $(m-1)N$ zeros padded.

Our first step is to find the interpolation coefficients x_ℓ which satisfy the following conditions:

$$s_k z^{kmc'_j} = \sum_{\ell=-q/2}^{q/2} x_\ell(c'_j) z^{k[mc'_j]+\ell} \tag{7}$$

where $z = e^{i2\pi/mN}$.

Through similar procedures as in [6], we can calculate the least-square solution of the coefficients as $x(c'_j) = F^{-1}a(c'_j)$ where $F = A^\dagger A$ is the regular Fourier matrix, and $a(c'_j) = A^\dagger v(c'_j)$. The matrix A, F and vector v are listed bellow:

$$A = \begin{pmatrix} 1 & 1 & \cdots & 1 \\ z^{[mc'_j]-q/2} & z^{[mc'_j]-q/2+1} & \cdots & z^{[mc'_j]+q/2} \\ \vdots & \vdots & \ddots & \vdots \\ z^{N([mc'_j]-q/2)} & z^{N([mc'_j]-q/2+1)} & \cdots & z^{N([mc'_j]+q/2)} \end{pmatrix}$$

$$F = \begin{pmatrix} N+1 & \dfrac{1-z^{N+1}}{1-z} & \cdots & \dfrac{1-z^{q(N+1)}}{1-z^q} \\ \dfrac{1-z^{-(N+1)}}{1-z^{-1}} & N+1 & \cdots & \dfrac{1-z^{(q-1)(N+1)}}{1-z^{q-1}} \\ \vdots & \vdots & \ddots & \vdots \\ \dfrac{1-z^{-q(N+1)}}{1-z^{-q}} & \dfrac{1-z^{-(q-1)(N+1)}}{1-z^{-(q-1)}} & \cdots & N+1 \end{pmatrix}$$

and

$$v(c'_j) = \begin{pmatrix} s_0 & s_1 z^{mc_j} & s_2 z^{2mc_j} & \cdots & s_N z^{Nmc_j} \end{pmatrix}^T$$

Here the regular Fourier matrix F is uniquely determined by (m, N, q) and is independent of c_j. This is the key point of our algorithm as it makes the interpolation efficient. For given parameters (m, N, q), the regular Fourier matrix need to be calculated only once, making the solution for the interpolating coefficients efficient.

Our second step is to find the solution to (6) by regular FFT. Equation (6) can be rewritten as:

$$\mu_j = \sum_{k=0}^{N} \beta_k e^{i2\pi kj}/mN, \qquad j = [mc_j] + \ell, \tag{8}$$

Then through (5), we obtain the sequence $\tilde{f}_j$ $(j = 0, 1, 2, \ldots, N)$, and hence the real part f_j.

Similarly, the NUFCT-2 algorithm for (2) consists of following steps:

1)Calculate the transform coefficients by

$$T_n = \sum_{\ell,k,[mc'_k]+\ell=n} \alpha_k x_\ell (c'_k)$$

2) Use the regular FFT to calculate the following equation:

$$\tilde{g}_j s_j = \sum_{n=0}^{mN} T_n e^{i2\pi nj/mN}$$

3) Scale the values by s_j.

The asymptotic number of arithmetic operations of these NUFCT algorithms is $O(2mN \log_2 N)$, where $m \ll N$. Usually we choose $q = 8$ and $m = 2$.

2.2 The Inverse Nonuniform Fast Cosine Transform (NUIFCT) Algorithms

Corresponding to the two forward NUFCT algorithms, we also developed two inverse algorithms, NUIFCT-1 and NUIFCT-2. These algorithms find α_k from f_j and g_j, respectively, with $O(N \log_2 N)$ arithmetic operations. In comparison, the direct solution requires $O(N^3)$ arithmetic operations.

Equation (1) can also be written as $f = B\alpha$. From the elementary matrix identities we know that $B^{-1} = (B^\dagger B)^{-1} B^\dagger$, so the solution to inverse DCT is

$$\alpha = (B^\dagger B)^{-1} h, \qquad h = B^\dagger f \tag{9}$$

where $B_{jk} = \cos \frac{k\pi c_j}{N}$. Note that $(B^\dagger B)_{j\ell} = \frac{1}{2}(a_{j+\ell} + b_{j-\ell})$ where

$$a_j = \sum_{k=0}^{N} \cos \frac{j\pi c_k}{N}, \qquad j = 0, 1, 2, \ldots, 2N$$

and

$$b_j = \sum_{k=0}^{N} \cos \frac{j\pi c_k}{N}, \qquad j = -N, -N+1, \ldots, N-1, N$$

which can be calculated by the NUFCT-2 algorithm with $O(N \log_2 N)$ arithmetic operations. Similarly, h in (9) can also be obtained by using NUFCT-2. Then the solution α in (9) can be obtained by using the conjugate-gradient FFT (CG-FFT) method [28, 29]. In the CG-FFT method, the solution of α is obtained iteratively. Each CG iteration involves operations such as discrete correlation and convolution

$$\sum_{\ell}(B^{\dagger}B)_{j\ell}y_{\ell} = \frac{1}{2}\left\{\mathcal{F}^{-1}[\mathcal{F}(a)\mathcal{F}^{*}(y) + \mathcal{F}(b)\mathcal{F}(y)]\right\}_j \tag{10}$$

where $\mathcal{F}$ represents the fast Fourier transform.

In summary, the procedures for the NUIFCT-1 algorithm are:

1) Calculate the array h by using NUFCT-2;
2) Find arrays a_j and b_j with NUFCT-2;
3) Solve α in (9) via the CG-FFT method.

Similarly, the representation of NUIFCT-2 can be written as:

$$f = B^{\dagger}\alpha$$

Then the solution of NUIFCT-2 is:

$$\alpha = (B^{\dagger})^{-1}f = B(B^{\dagger}B)^{-1}f = Bd, \qquad d = (B^{\dagger}B)^{-1}f$$

After using CG-FFT to calculate d, the transform coefficients can be easily obtained by using NUFCT-1.

2.3 Application of NUFCT in the Chebyshev PSTD Algorithm

One of many applications of the NUFCT algorithms is the solution of Maxwell's equations by the Chebyshev PSTD method. Maxwell's equations governing the electric and magnetic fields in the medium with permeability μ, electric permittivity ϵ and conductivity σ are given as:

$$\nabla \times \mathbf{E} = -\mu\frac{\partial \mathbf{H}}{\partial t} - \mathbf{M} \tag{11}$$

$$\nabla \times \mathbf{H} = \epsilon\frac{\partial \mathbf{E}}{\partial t} + \mathbf{J} + \sigma\mathbf{E} \tag{12}$$

where $\mathbf{J}$, $\mathbf{M}$ are the imposed electric and magnetic current densities, respectively. The conventional method to solve these equations is the

finite-difference time-domain method [9–11]. Here we use the NUFCT algorithms to approximate the spatial derivatives and solve equations (11) and (12) by a leap-frog scheme. We demonstrate the nonuniform Chebyshev PSTD method through a one-dimensional problem.

For a one-dimensional TEM wave propagating along the x direction, the above equations become

$$\frac{\partial E_y(x,t)}{\partial x} = -\mu \frac{\partial H_z(x,t)}{\partial t} - M_z(x,t) \tag{13}$$

$$-\frac{\partial H_z(x,t)}{\partial x} = \epsilon \frac{\partial E_y(x,t)}{\partial t} + J_y(x,t) + \sigma E_y(x,t). \tag{14}$$

To truncate the computation domain, we use the perfect matched layer (PML) as the absorbing boundary condition [19] under complex coordinates [20, 30, 31]

$$e_\eta = a_\eta + i\frac{\omega_\eta}{\omega}, \qquad \eta = x, y, z.$$

In frequency domain, we replace the operator ∇ in Maxwell's equations by

$$\nabla_e = \sum_{\eta=x,y,z} \hat{\eta} \frac{1}{e_\eta} \frac{\partial}{\partial \eta}$$

Then in time domain equation (13) and (14) become:

$$a_y \epsilon \frac{\partial E_y(x,t)}{\partial t} + (a_y \sigma + \omega_y \epsilon) E_y(x,t) + \omega_y \sigma \int_{-\infty}^{t} E_y(x,t)dt = -\frac{\partial H_z(x,t)}{\partial x} - J_y(x,t) \tag{15}$$

$$a_z \mu \frac{\partial H_z(x,t)}{\partial t} + \omega_z \mu H_z(x,t) = -\frac{\partial E_y(x,t)}{\partial x} - M_z(x,t). \tag{16}$$

In the above, a_η and ω_η are respectively the scaling and attenuation factors of the PML. In a regular region of interest, $a_\eta = 1$ and $\omega_\eta = 0$; while in the PML region surrounding the region of interest $a_\eta \geq 1$ and $\omega_\eta > 0$. The outer boundary of the PML region may assume the condition of a perfect electric or magnetic conductor.

For the time integration of the (15) and (16), we use the center differencing scheme with a temporal staggered grid. Here, the **H** field

is defined at $(n+1/2)\Delta t$ whereas the **E** field is defined at $n\Delta t$. The temporal derivatives are approximated by central difference which has the second-order accuracy. Following the same procedure as in [31], we achieve the time-stepping equations for **E** field and **H** field as:

$$H_z(x, n+1/2) = \frac{\left(\frac{a_x\mu}{\Delta t} - \frac{\omega_x\mu}{2}\right) H_z(x, n-1/2) - \frac{\partial E_y(x,n)}{\partial x} - M_z(x,n)}{a_x\mu/\Delta t + \omega_x\mu/2} \tag{17}$$

$$E_y(x, n+1) = \frac{\left(\frac{a_x\epsilon}{\Delta t} - \frac{\omega_x\epsilon}{2} - \frac{\sigma}{2}\right) E_y(x,n) - \omega_y\sigma E_y^I - \frac{\partial H_z(x,n+1/2)}{\partial x} - J_y\left(x, n+\frac{1}{2}\right)}{a_x\epsilon/\Delta t + \omega_x\epsilon/2 + \sigma/2} \tag{18}$$

where $E_y^I = \int_{-\infty}^{t} E_y dt$ is the time-integrated electric field.

In order to use the NUFCT algorithms for the spatial derivatives, we expand the electric and magnetic field by the Chebyshev polynomials. For example, a function $f(y)(y \in [1,1])$ can be approximated as:

$$f(y) = \sum_{k=0}^{N} \alpha_k T_k(y) \tag{19}$$

where $T_k = \cos(k\cos^{-1}(y))$ is the kth Chebyshev polynomial. To find the coefficients α, we multiply T_m on both sides of equation (19) and integrate over y from -1 to 1,

$$\int_{-1}^{+1} \frac{f(y)T_m(y)dy}{\sqrt{1-y^2}} = \sum_{k=0}^{N} \alpha_k \int_{-1}^{+1} \frac{T_k(y)T_m(y)dy}{\sqrt{1-y^2}}$$

Applying the orthogonality of Chebyshev polynomials, we obtain the representation of α_k as:

$$\alpha_k = \frac{2-\delta_{k0}}{\pi} \int_{-1}^{+1} \frac{f(y)T_k(y)dy}{\sqrt{1-y^2}} \doteq \frac{2-\delta_{k0}}{N} (-1)^k \sum_{j=0}^{N} f(y_j)\cos(k\pi c_j/N)\Delta c_j \tag{20}$$

In equation (20), we set $y = -\cos\left(\frac{\pi c}{N}\right)$, $c \in [0, N]$ and δ_{kj} is the Kronecker delta function. It is efficient to calculate α by using our NUFCT-2 algorithm. From equation (20), it is also obvious that we can use the regular FCT algorithm to compute α_k if we let the value of y to locate at the extrema points of Chebyshev polynomials $y = -\cos(\pi j/N)$, $j = 1, 2, \ldots, N$. In the nonuniform case, c_j are any real numbers within $[0, N]$.

Similarly, the spatial derivative df/dx can also be expanded in terms of Chebyshev polynomials:

$$\frac{df(y)}{dy} = \frac{d}{dy}\sum_{k=0}^{N}\alpha_k T_k(y) = \sum_{k=0}^{N}\beta_k T_k(y) \tag{21}$$

From the recursion relation for the first derivative of Chebyshev polynomials

$$\frac{T'_{n+1}}{n+1} - \frac{T'_{n-1}}{n-1} = 2T_n,$$

it is straightforward to get the relation between the coefficients α_k and β_k in (21). Specifically, equation (21) can be written as:

$$\alpha_0 T'_0 + \alpha_1 T'_1 + \cdots + \alpha_N T'_N = \beta_0 T'_1 + \frac{\beta_1}{4} T'_2 + \cdots + \frac{\beta_N}{2}\left(\frac{T'_{N+1}}{N+1} - \frac{T'_{N-1}}{N-1}\right)$$

Comparing the coefficients of the same Chebyshev polynomials, we obtain β_k from the given coefficients α_k from the following relations:

$$\begin{aligned}
\beta_N &= 0 \\
\beta_{N-1} &= 2N\alpha_N \\
\beta_{N-2} &= 2(N-1)\alpha_{N-1} \\
\beta_{i-1} &= \beta_{i+1} + 2i\alpha_i, \qquad i = N-2,\ N-3, \ldots, 2 \\
\beta_0 &= \alpha_1 + \beta_2/2
\end{aligned}$$

Once β_k are found, the spatial derivative of $\frac{df(y)}{dy}$ can be obtained very efficiently with the NUFCT-1 algorithm.

In the above derivation of the derivative using Chebyshev polynomials, we have assumed that $y \in [-1, 1]$. However, we can apply it to any computational domain by a simple linear transformation. For given domain $x \in [x_1, x_2]$, we define $x = ay + b$, where

$y \in [-1, 1]$, $a = (x_2 - x_1)/2$ and $b = (x_2 + x_1)/2$. Thus the derivative of $f(x)$ is:

$$\frac{df(x)}{dx} = \frac{df(ay+b)}{dy}\frac{dy}{dx} = \frac{1}{a}\frac{df(ay+b)}{dy}.$$

Given the approximation of the derivatives, equations (17) and (18) form a leap-frog system on a centered grid where all field components are defined at the cell centers. Thus, either from the initial conditions of the fields or from the continuous source excitation, the fields at all later time steps can be obtained.

3. NUMERICAL RESULTS

3.1 Numerical Results of NUFCT Algorithms

For our forward NUFCT algorithms, we select $N = 64$, $m = 2$ and $q = 8$ for the following examples. The input data $\{\alpha_k\}$ and the sampling intervals are obtained by a pseudorandom number generator with a uniform distribution within the range of [0, 1]. Fig. 1(a) compares the NUFCT-1 output data with the results evaluated by the direct sum. Fig. 1(b) shows the absolute error between the NUFCT and direct results. The NUFCT algorithm has the L_2 and L_∞ errors [4] of $E_2 = 1.2760 \times 10^{-6}$ and $E_\infty = 8.07 \times 10^{-6}$. In Fig. 2, we compare the numbers of arithmetic operations in our NUFCT-1 algorithm with the theoretical behavior. It is clear that our algorithm has the complexity of $O(N \log_2 N)$.

For the inverse algorithm NUIFCT-1, we use the same parameters $N = 64$, $m = 2$, $q = 8$. The input data are also randomly distributed within [0, 1]. Fig. 3(a) shows the comparison of NUIFCT-1 result and direct result. Fig. 3(b) is the absolute error. Here the L_2 and L_∞ errors are $E_2 = 8.3375 \times 10^{-5}$ and $E_\infty = 2.76 \times 10^{-5}$. From Fig. 4, we show that our NUIFCT algorithm has the complexity of $O(N \log_2 N)$. Since the NUFCT-2 and NUIFCT-2 have a similar accuracy as the NUFCT-1 and NUIFCT-1, their results are omitted for brevity.

3.2 Numerical Results of One-Dimensional Chebyshev PSTD Algorithm

First we show the NUFCT algorithm for the derivative of the function. In this example, the function $f(x)$ is the first derivative of the Balckman-Harris window function. Using $N = 16$ in the NUFCT

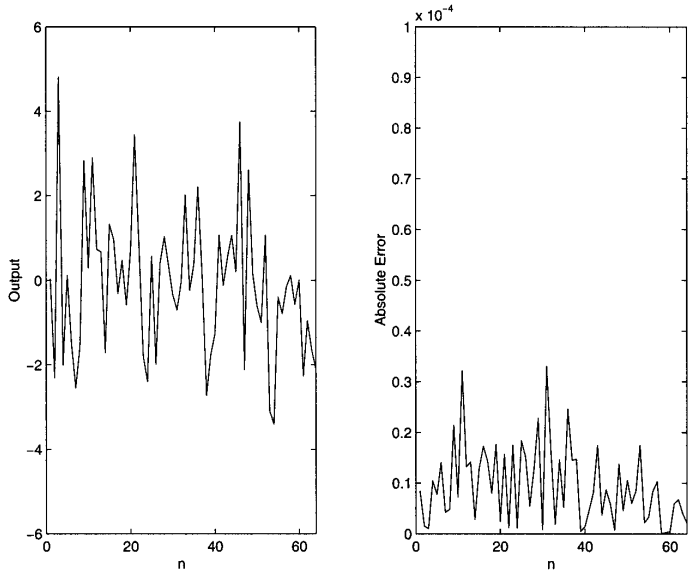

(a) (b)

Figure 1. (a) Comparison of the NUFCT-1 output data with the direct evaluated results. (b) The absolute error of the NUFCT results.

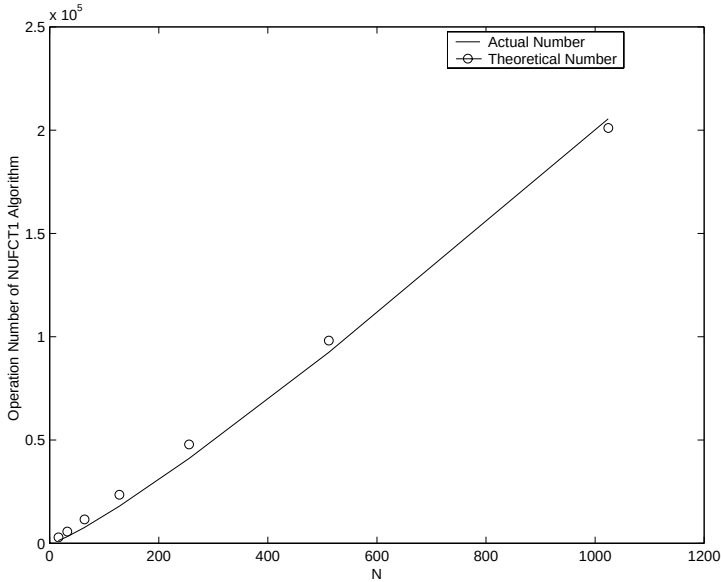

Figure 2. Number of arithmetic operations as a function of N in the NUFCT-1 algorithm. The theoretical curve is proportional to $O(N \log_2 N)$.

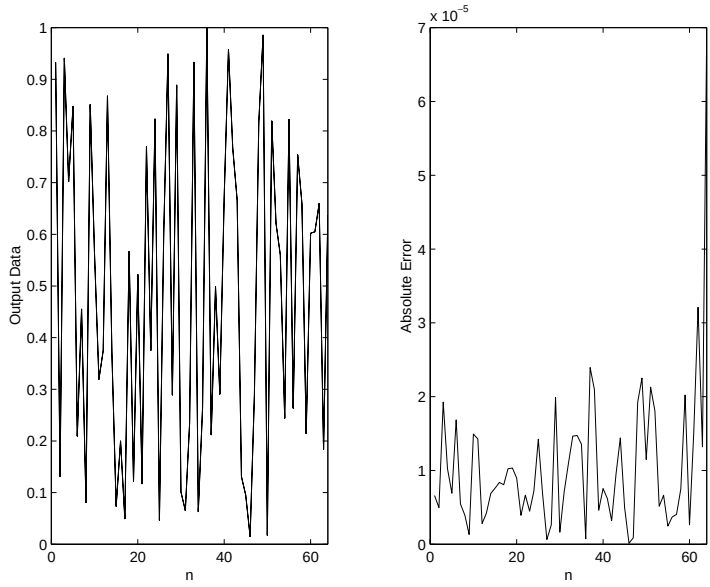

(a) (b)

Figure 3. (a) Comparison of the NUIFCT-1 output data with the direct evaluated results. (b) The absolute error of the NUIFCT results.

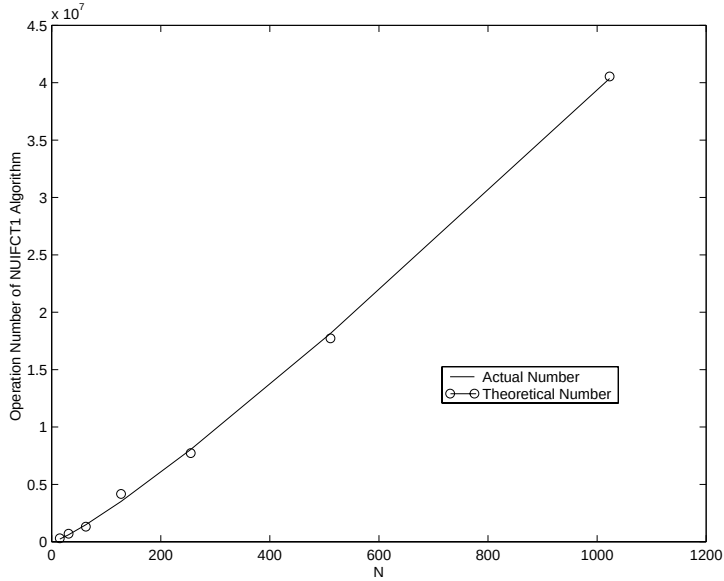

Figure 4. Number of arithmetic operations as a function of N. The theoretical curve is proportional to $O(N \log_2 N)$.

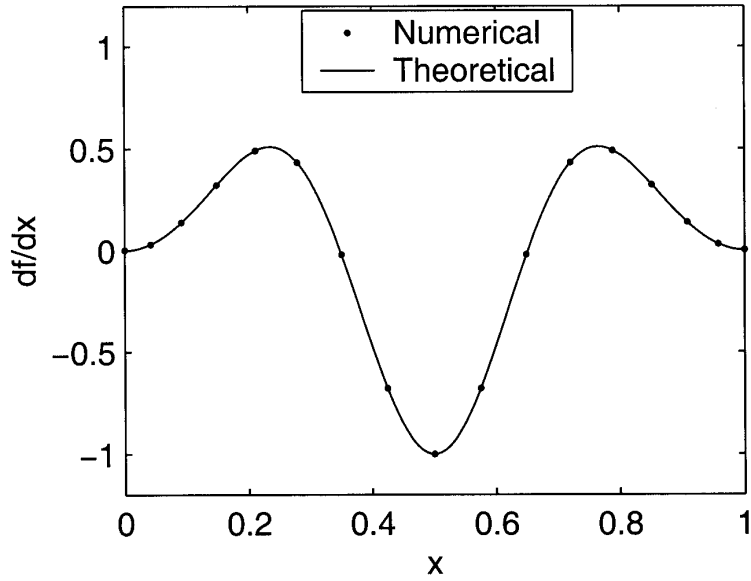

Figure 5. The Numerical derivative df/dx on a nonuniform grid by the NUFCT algorithm $(N = 16)$ along with the exact solution.

algorithm with a nonuniform grid, the numerical derivative df/dx is compared with the exact solution in Fig. 5.

We used the Chebyshev PSTD algorithm to simulate electromagnetic wave propagation in both homogeneous and inhomogeneous media. An electric current source is used to excite the electromagnetic waves. Its time function is the first derivative of Blackman-Harris window function with a center frequency $f_c = 200\,\text{MHz}$.

The first case is free space. The computation domain is [0, 12] with only 64 uniformly distributed points. Therefore, the sampling density is π cells per wavelength at $f = 2.5 f_c$. The source is located in the center of medium and receivers are distributed among the whole region to measure the **E** field. Fig. 6 shows the comparison of cell size Δx_j used here and the cell size used in the Chebyshev PS method. Fig. 7 compares the **E** field with the analytical solution at all receivers while Fig. 8 shows the comparison of one receiver. The numerical result agree well with the analytical solution.

In an inhomogeneous case, we have a two-layer medium: free space from $x = 0\,\text{m}$ to $x = 8\,\text{m}$ and medium with $\epsilon_r = 4$, $\mu_r = 1$, $\sigma = 0$ from 8 m to 12 m. The dipole is placed at the center of free space.

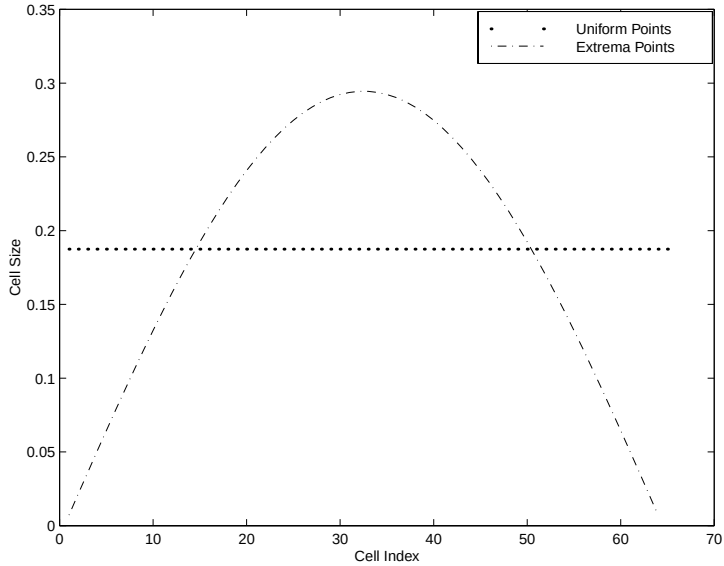

Figure 6. The comparison of cell size Δx_j for the uniform distribution and the conventional distribution at extrema points of Chebyshev polynomials.

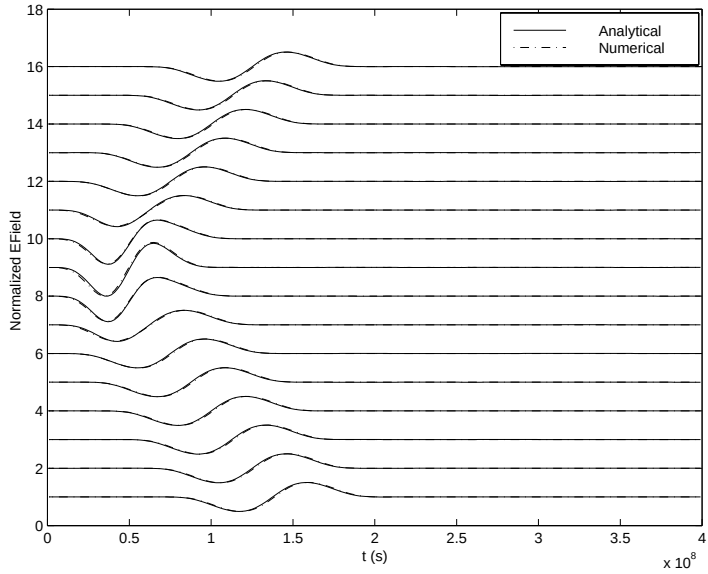

Figure 7. The normalized E-field at every 4th grid point.

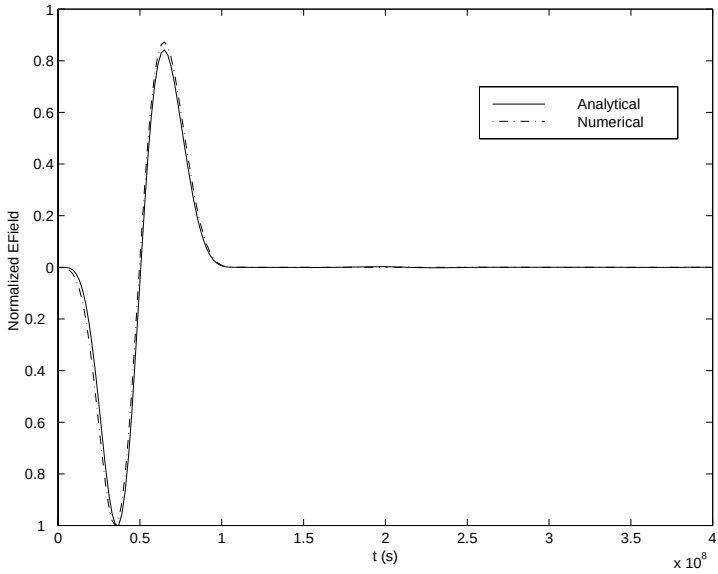

Figure 8. The comparison of normalized E-field at one receiver.

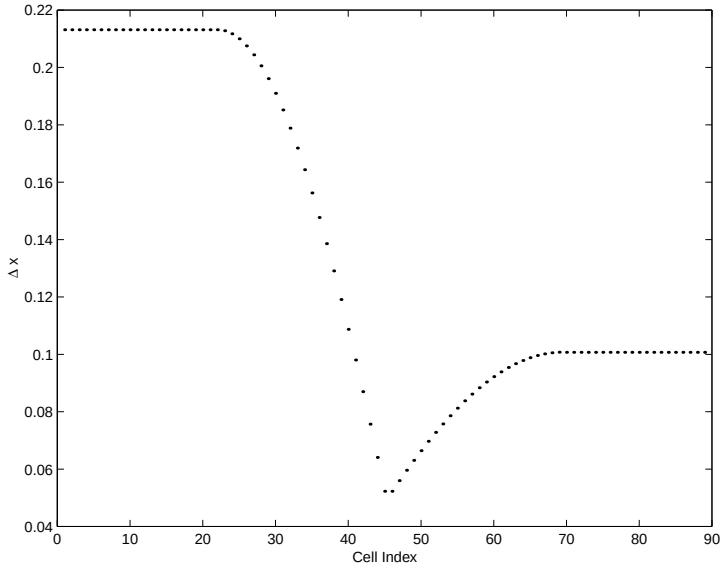

Figure 9. The cell size Δx_j as a function of the cell index.

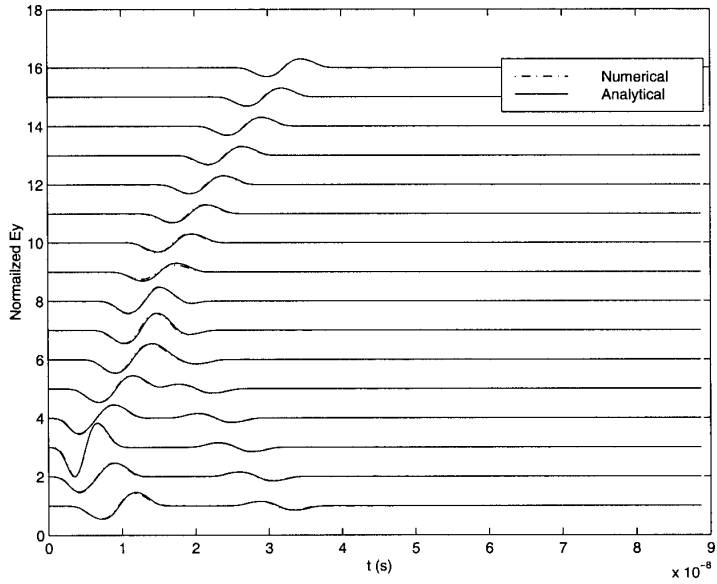

Figure 10. The comparison of normalized E-field at all receivers in the inhomogeneous case.

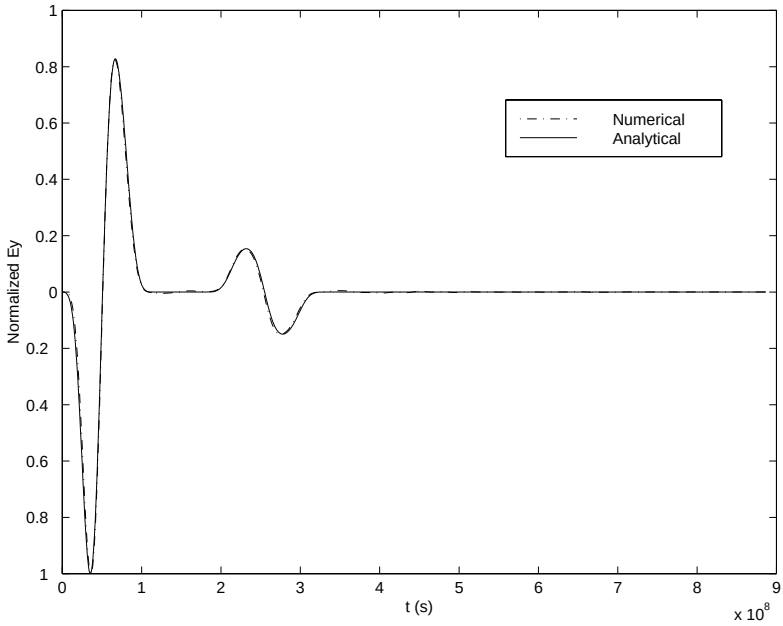

Figure 11. The comparison of normalized E-field at one receiver.

Here we use 88 points, also about π cells per wavelength. Fig. 9 shows the cell size as a function of x. We have selected denser points around the boundary to reduce the Gibbs' phenomenon and uniform cells elsewhere. Fig. 10 is the comparison of **E** field at all receivers and Fig. 11 compares results at one receiver. The agreement is also very good.

4. CONCLUSIONS

Using the least-squares interpolation and the regular Fourier matrix, we develop nonuniform fast forward cosine transform (NUFCT) algorithms for nonuniformly spaced data. Based on forward algorithms and CG-FFT, we also propose nonuniform inverse fast cosine transform (NUIFCT) algorithms. Numerical results show that these NUFCT algorithms are very accurate and require only $O(N \log_2 N)$ arithmetic operations.

NUFCT algorithms are used in the Chebyshev PSTD algorithm to allow an nonuniform grid so that the grid points need not locate at the extrema points of Chebyshev polynomials. This property is very useful for inhomogeneous media and enables us to take all layers of medium within one region. As long as we select more points around each boundary and satisfy π cells per wavelength on the average, the numerical results agree well with analytical results. However, without NUFCT, we would have to calculate the fields with a multiregion scheme and match these solutions at the interfaces between regions. Multidimensional results of the Chebyshev PSTD method will be reported in the near future.

ACKNOWLEDGMENT

This work was supported by Environmental Protection Agency through a PECASE grant CR-825-225-010, and by the National Science Foundation through a CAREER grant ECS-9702195.

REFERENCES

1. Rao, K. R., and P. Yip, *Discrete Cosine TransformAlgorithms, Advantages, Applications,* Academic Press, London, 1990.
2. Chen, W. A., C. Harrison, and S. C. Fralick, "A fast computational algorithm for the discrete cosine transform," IEEE Trans. Commu., Vol. 25, No. 9, 1004–1011, 1977.
3. Lee, B. G., "A new algorithm to compute the discrete cosine transform," *IEEE Trans. Acoust., Speech, Signal Processing,* Vol. ASSP-32, No. 6, 1243–1245, 1984.
4. Dutt, A., and V. Rokhlin, "Fast Fourier transforms for nonequispaced data," *SIAM J. Sci. Comput.,* Vol. 14, No. 6, 1368–1393, November 1993.
5. Beylkin, G., "On the fast Fourier transform of functions with singularities," *Appl. Computat. Harmonic Anal.,* Vol. 2, 363–382, 1995.
6. Liu, Q. H., and N. Nguyen, "An accurate algorithm for nonuniform fast Fourier transforms," *IEEE Microwave Guided Wave Lett.,* Vol. 8, No. 1, 18–20, 1998.
7. Liu, Q. H., and X. Y. Tang, "Iterative algorithm for nonuniform inverse fast Fourier transform (NU-IFFT)," *Electronics Letters,* Vol. 34, No. 20, 1913–1914, 1998.
8. Nguyen, N., and Q. H. Liu, "The regular Fourier matrices and nonuniform fast Fourier transforms," *SIAM J. Sci. Compt.,* Vol. 21, No. 1, 283–293, 1999.
9. Yee, K. S., "Numerical solution of initial boundary value problems involving Maxwell's equations in isotropic media," *IEEE Trans. Antennas Propagat.,* Vol. AP-14, 302–307, 1966.
10. Kunz, K. S., and R. J. Luebbers, *Finite Difference Time Domain Method for Electromagnetics,* CRC Press Inc., Florida, 1993.
11. Taflove, A., *Computational Electrodynamics: The Finite Difference Time Domain Method,* Artech House, Inc., Norwood, MA, 1995.
12. Fang, J., "Time domain finite difference computation for Maxwell's equations," Ph.D. dissertation, University of California, Berkeley, CA, 1989.
13. Hadi, M. F., and M. Piket-May, "A modified FDTD (2,4) scheme for modeling electrically large structures with high phase accuracy," *12th Annu. Rev. Progress Appl. Computat. Electromagnet.,* Monterey, CA, March 1996.
14. Carpenter, M. H., D. Gottlieb, and S. Abarbanel, "The stability of numerical boundary treatments for compact higher-order finite difference schemes," *Inst. Comput. Applicat. Sci. Eng.,* Rep. 91-71, 1991.

15. Young, J. L., D. Gaitonde, and J. J. S. Shang, "Toward the construction of a fourth-order difference scheme for transient EM wave simulation: staggered grid approach," *IEEE Trans. Antennas Propagat.,* Vol. 45, No. 11, 1573–1580, 1997.
16. Orszag, S. A., "Comparison of pseudospectral and spectral approximation," *Stud. Appl. Math.,* Vol. 51, 253–259, 1972.
17. Gottlieb, D., and S. A. Orszag, *Numerical Analysis of Spectral Methods,* SIAM, Philadelphia, 1977.
18. Fornberg, B., *A Practical Guide to Pseudospectral Methods,* Cambridge University Press, New York, 1996.
19. Berenger, J.-P., "A perfectly matched layer for the absorption of electromagnetic waves," *J. Computational Physics,* Vol. 114, 185–200, 1994.
20. Liu, Q. H., "The PSTD algorithm: a time-domain method requiring only two cells per wavelength," *Microwave Opt. Tech. Lett.,* Vol. 15, No. 3, 158–165, 1997.
21. Liu, Q. H., "Large-scale simulations of electromagnetic and acoustic measurements using the pseudospectral time-domain (PSTD) algorithm," *IEEE Trans. Geosci. Remote Sensing,* Vol. 37, No. 2, 917–926, 1999.
22. Liu, Q. H., "PML and PSTD algorithm for arbitrary lossy anisotropic media," *IEEE Microwave Guided Wave Lett.,* Vol. 9, No. 2, 48–50, 1999.
23. Liu, Q. H., and G.-X. Fan, "A frequency-dependent PSTD algorithm for general dispersive media," *IEEE Microwave Guided Wave Lett.,* Vol. 9, No. 2, 51–53, 1999.
24. Liu, Q. H., and G.-X. Fan, "Simulations of GPR in dispersive media using the PSTD algorithm," *IEEE Trans. Geosci. Remote Sensing,* Vol. 37, No. 5, 2317–2324, 1999.
25. Liu, Q. H., "The PSTD algorithm for acoustic waves in inhomogeneous, absorptive media," *IEEE Trans. Ultrason., Ferroelect., Freq. Contr.,* Vol. 45, No. 4, 1044–1055, 1998.
26. Yang, B., D. Gottlieb, and J. S. Hesthaven, "On the use of PML ABC's in spectral time-domain simulations of electromagnetic scattering," *Proc. ACES 13th Annual Review of Progress in Applied Computational Electromagnetics,* Monterey, 926–933, 1997.
27. Yang, B., D. Gottlieb, and J. S. Hesthaven, "Spectral simulations of electromagnetic waves scattering," *J. Comp. Phys.,* Vol. 134, 216–230, 1997.
28. Sarkar, T. K., "Application of conjugate gradient method to electromagnetics and signal analysis," *PIER 5, Progress in Electromagnetics Research,* Elsevier, New York, 1991.

29. Catedra, M. F., and R. P. Torres, *J. Basterrechea, and E. Gago, The CG-FFT Method: Application of Signal Processing Techniques to Electromagnetics,* Boston: Artech House, 1995.
30. Chew, W. C., and W. H. Weedon, "A 3D perfectly matched medium from modified Maxwell's equations with stretched coordinates," *Microwave Opt. Tech. Lett.,* Vol. 7, 599–604, 1994.
31. Liu, Q. H., "An FDTD algorithm with perfectly matched layers for conductive media," *Micro. Opt. Tech. Lett.,* Vol. 14, No. 2, 134–137, 1997.